Supporting Information

Rationally Synthesis of IR820-Albumin Complex for NIR-II Fluorescence Imaging-guided Surgical Treatment of Tumors and Gastrointestinal Obstruction

Xinyu Feng,[†,#] Yuan Cao,[†,#] Pengrui Zhuang,[§] Ran Cheng,[†] Xuejun Zhang,[†] Hong Liu,[*,‡] Guohe Wang,[*,†] and Shao-Kai Sun[*,†]

[†]School of Medical Imaging, Tianjin Medical University, Tianjin 300203, China
[‡]The Second Surgical Department of Breast Cancer, Tianjin Medical University Cancer Institute and Hospital, National Clinical Research Center for Cancer, Key Laboratory of Cancer Prevention and Therapy, Tianjin's Clinical Research Center for Cancer, Tianjin 300060, China
[§]Department of Radiology, The Second Hospital of Tianjin Medical University, Tianjin 300211, China

*Corresponding Author: shaokaisun@tmu.edu.cn
wangguohe@tmu.edu.cn
liuhongzhang0101@163.com

TABLE OF CONTENTS

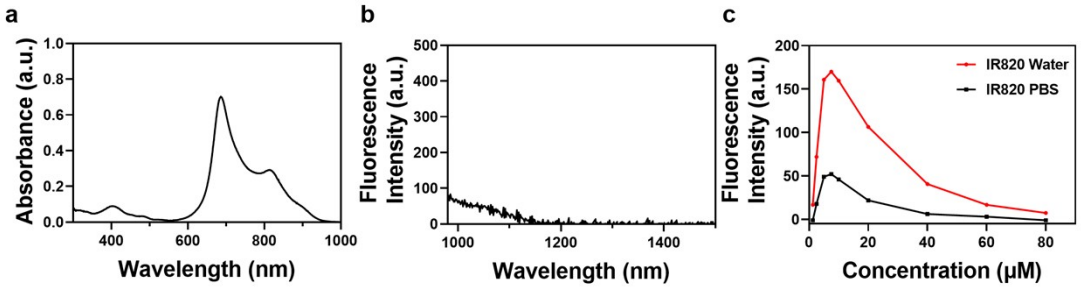

Figure S1. (a) The absorption spectrum of IR820. (b) The NIR-II fluorescence spectrum of IR820. (c) The NIR-II fluorescence intensity of IR820 with different concentrations in ultrapure water and PBS.

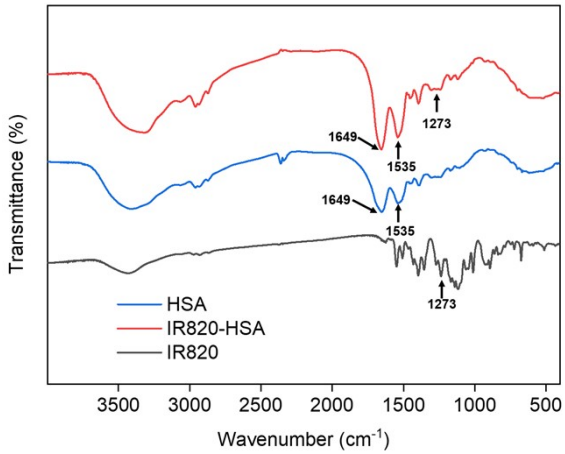

Figure S2. FT-IR spectra of IR820, HSA and IR820-HSA.

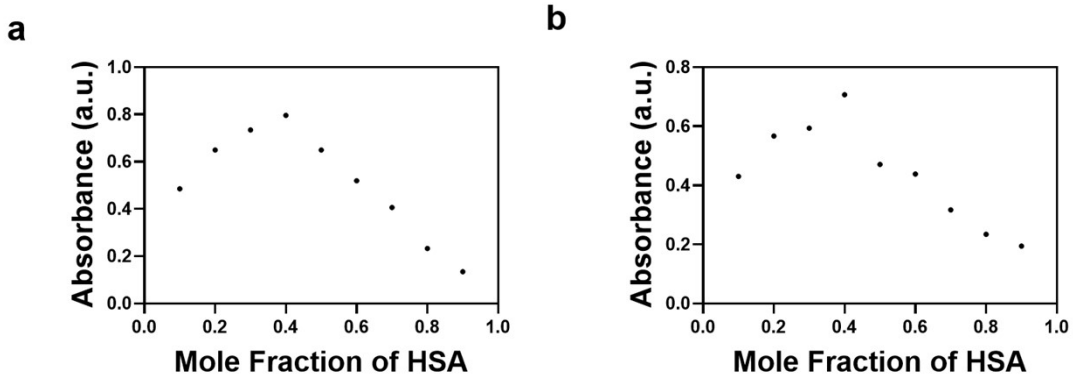

Figure S3. Job's plots of the IR820-HSA complex in (a) pH 2.4 buffer solution and (b) pH 7.4 buffer solution.

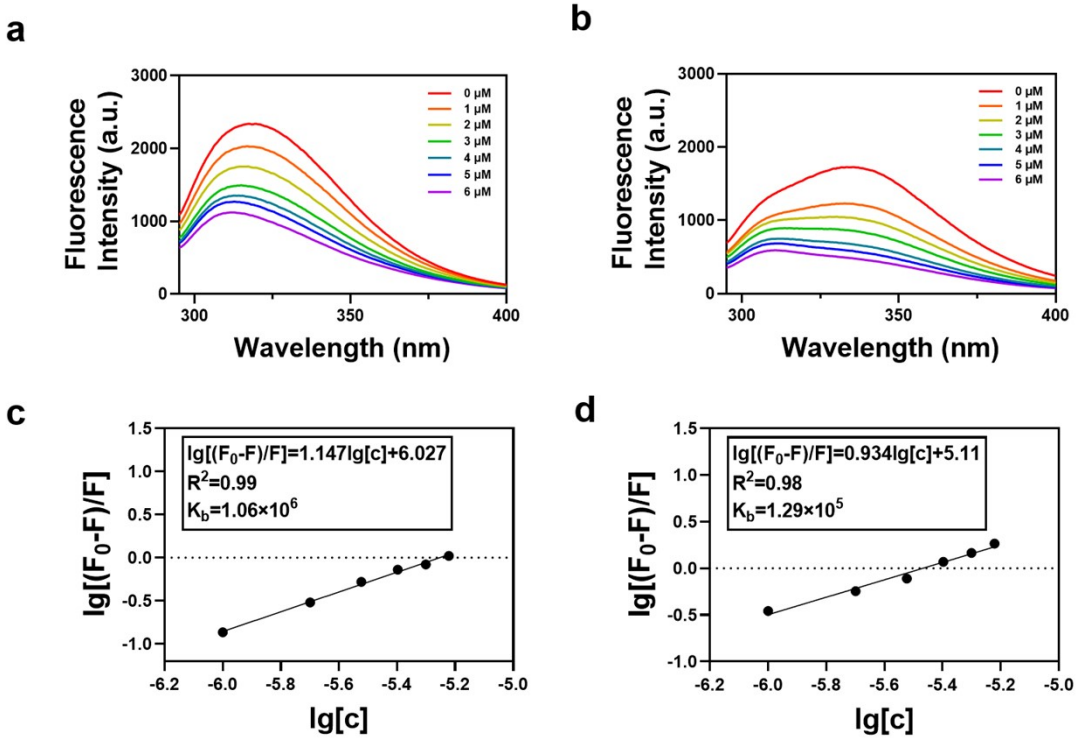

Figure S4. Fluorescence spectra of HSA with increasing concentration of IR820 (0−6 μM) in (a) buffer solution (pH 2.4) and (b) buffer solution (pH 7.4). The modified Stern-Volmer plots for quenching of HSA fluorescence by IR820 at 298 K in (c) buffer solution (pH 2.4) and (b) buffer solution (pH 7.4).

To obtain the proper fluorescence intensity values, fluorescence data were corrected for the inner filter effect according to the following equation.

$$F_{corr} = F_{obs} \times 10^{\frac{A_{ex} + A_{em}}{2}} \quad (1)$$

where F_{corr} and F_{obs} are corrected and observed fluorescence intensities, respectively. The absorbance of the solution at excitation and emission wavelengths is shown by A_{ex} and A_{em}, respectively. In all emission spectral scanning, both λ_{ex} and λ_{em} slit widths were set to 10.0 nm, and λ_{ex} and λ_{em} were set to 280 nm and 330 nm, respectively. The HSA concentration was maintained at 3 μM. Different concentrations of IR820 (0, 1, 2, 3, 4, 5, 6 μM) were added to quench the fluorescence of HSA at 330 nm. Binding constant (K_b) and binding stoichiometry (n) of the IR820-HSA complex were analyzed using the Stern−Volmer equation.[1,2]

$$lg[\frac{F_0 - F}{F}] = lgK_b + nlg[c] \quad (2)$$

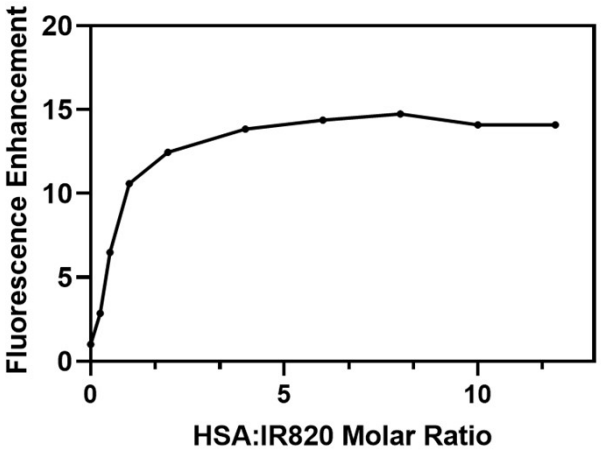

Figure S5. Fluorescence intensity enhancement of IR820-HSA with different HSA: IR820 molar ratios.

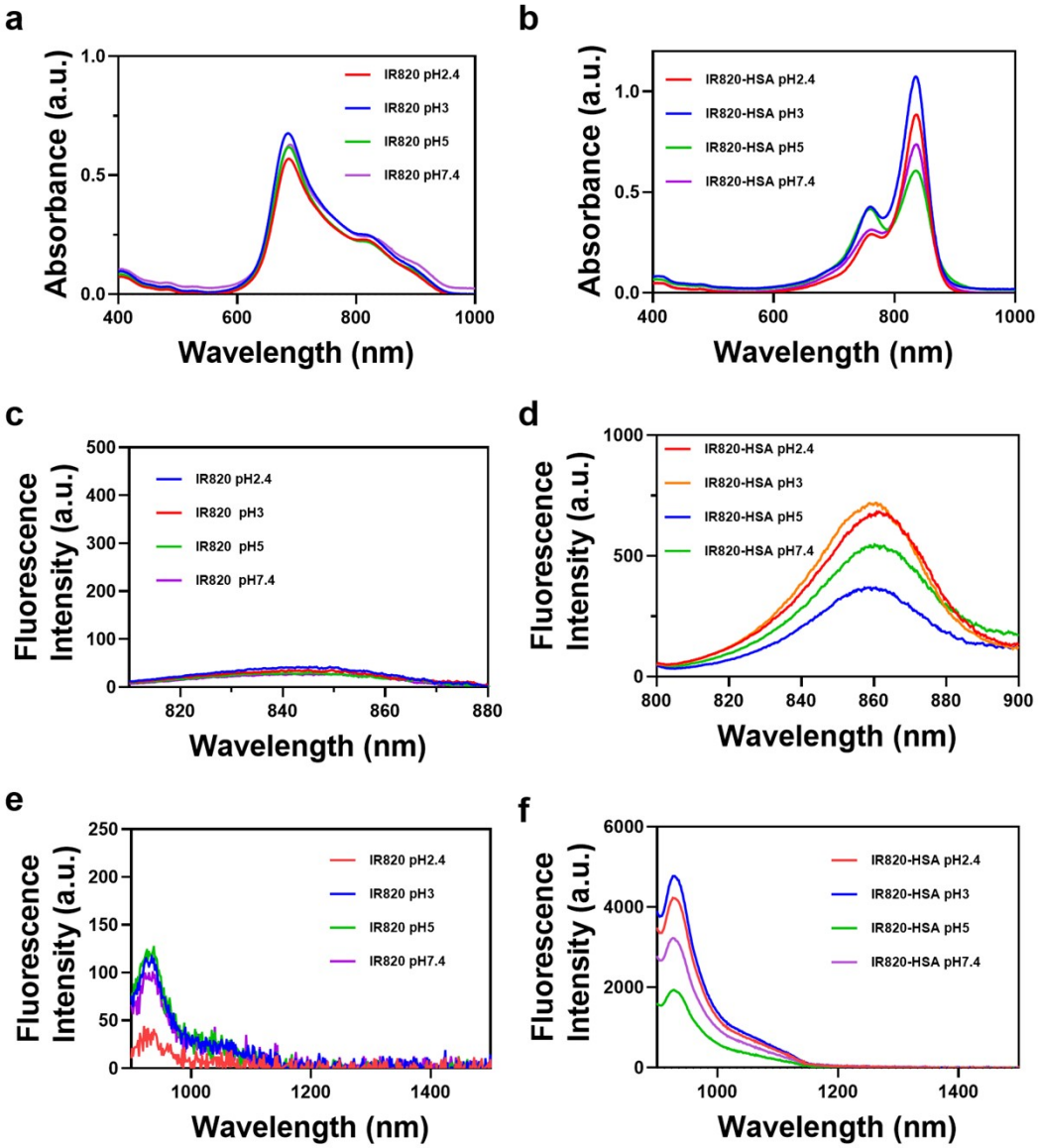

Figure S6. Absorption spectra in different pH conditions (pH 2.4, pH 3, pH 5, pH 7.4) of (a) IR820 and (b) IR820-HSA. NIR-I fluorescence emission spectra in different pH conditions (pH 2.4, pH 3, pH 5, pH 7.4) of (c) IR820 and (d) IR820-HSA. NIR-II fluorescence emission spectra in different pH conditions (pH 2.4, pH 3, pH 5, pH 7.4) of (e) IR820 and (f) IR820-HSA.

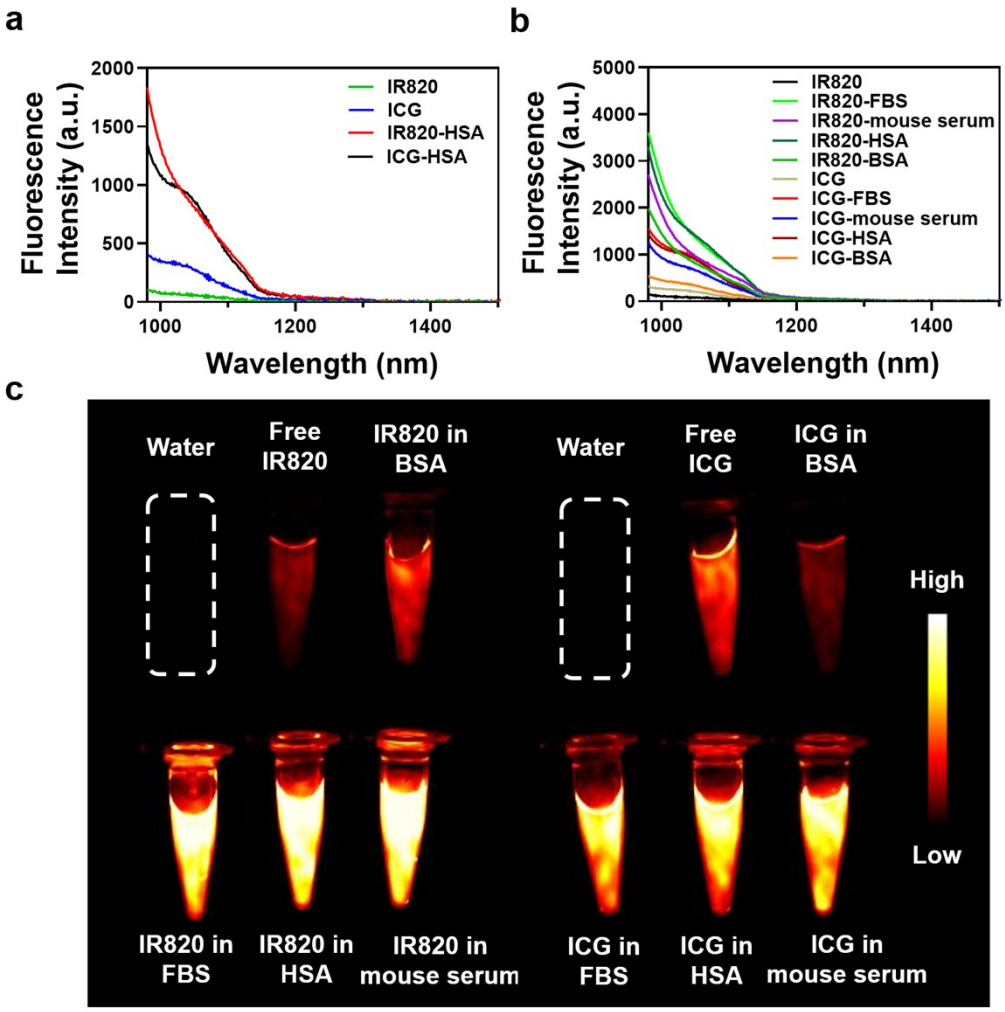

Figure S7. (a) The NIR-II fluorescence intensity of free IR820, ICG, IR820-HSA, ICG-HSA (molar ratio of IR820 or ICG to HSA, 1: 2). (b) The NIR-II fluorescence intensity of free IR820, free ICG, IR820 and ICG dissolved in high concentrations of albumin (40 mg/mL BSA, 40 mg/mL HSA, FBS, mouse serum). (c) The NIR-II fluorescence imaging of free IR820, free ICG, IR820 and ICG dissolved in high concentrations of albumin (40 mg/mL BSA, 40 mg/mL HSA, FBS, mouse serum).

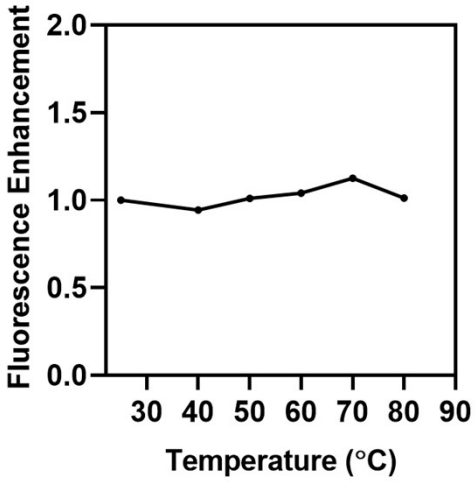

Figure S8. Fluorescence intensity increment of IR820-HSA complex after heated at different temperatures

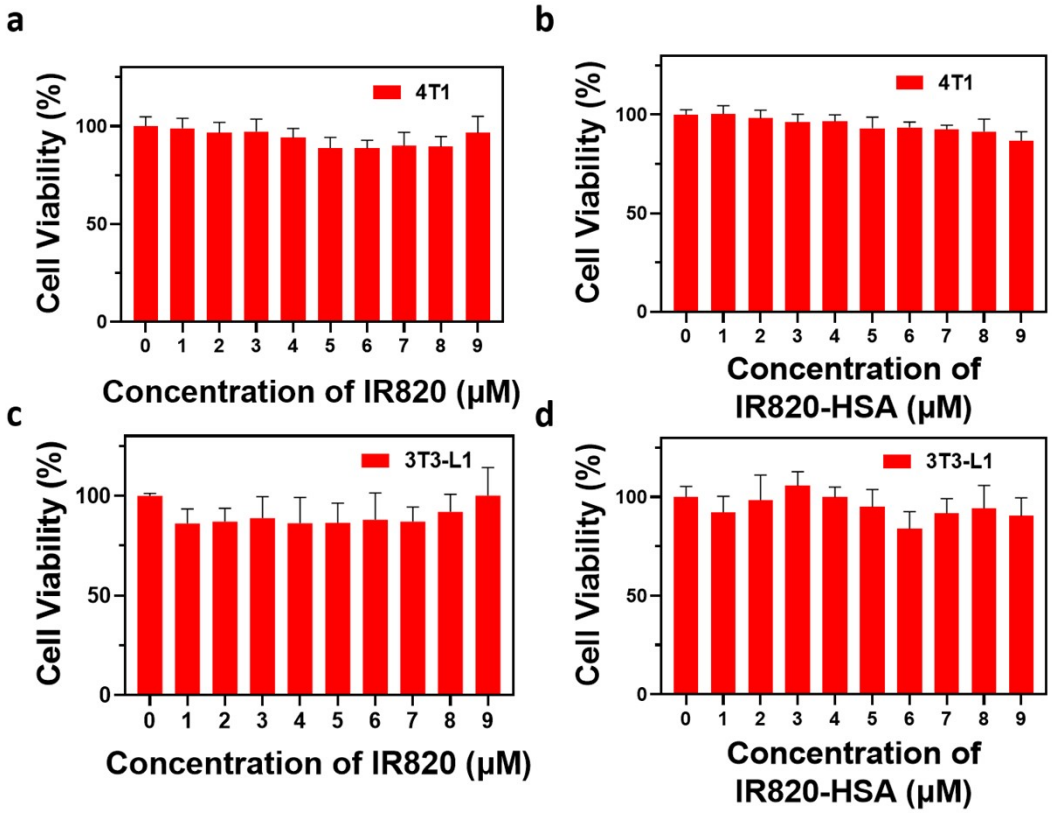

Figure S9. Cytotoxicity assay of IR820 and IR820-HSA. Cellular viability in (a) 4T1 cells and (c) 3T3-L1 cells after being treated with different concentrations of IR820. Cellular viability in (b) 4T1 cells and (d) 3T3-L1 cells after being treated with different concentrations of IR820-HSA.

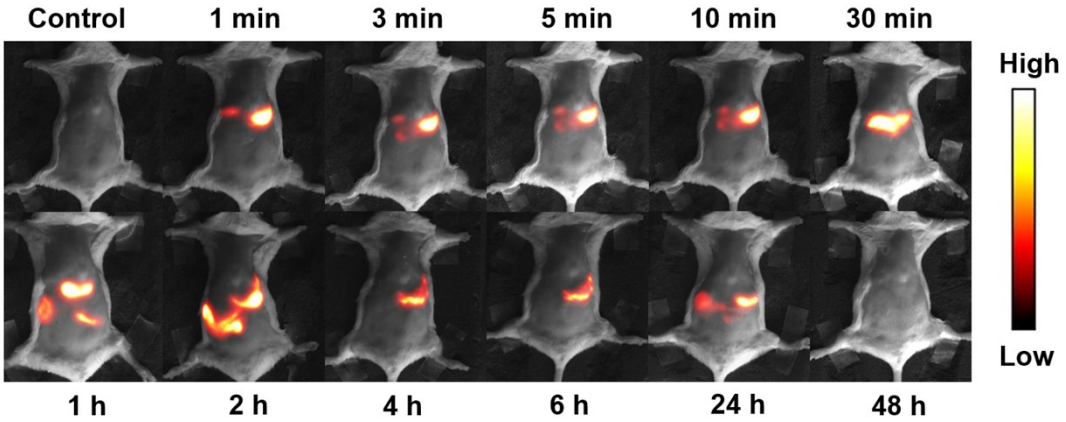

Figure S10. The NIR-II images of the digestive tract after oral administration of free IR820 at different time points (1000 ms, 58 mW/cm^2).

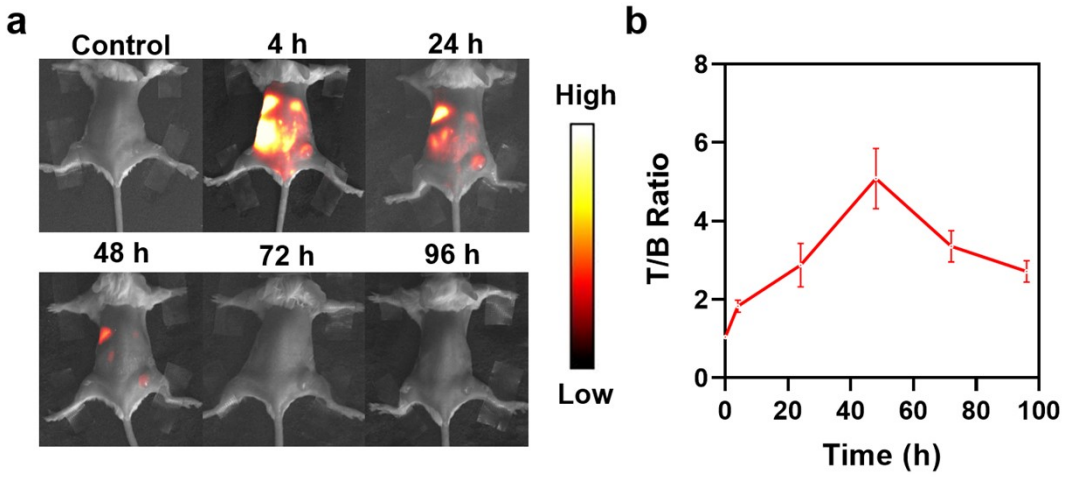

Figure S11. (a) The NIR-II images and (b) the tumor-to-background (T/B) ratios of 4T1-bearing mice injected with IR820-HSA (150 μL, 75 μM) through the tail vein at different time points (means ± SD, n = 3).

References

(1) Z. X. Chi and R. T. Liu, *Biomacromolecules*, 2011, **12**, 203-209.

(2) M. M. Puchalski, M. J. Morra and R. V. Wandruszka, *Fresenius J. Anal. Chem*. 1991, **340**, 341-344.